J Therm Anal Calorim (2011) 104:1005–1015
DOI 10.1007/s10973-010-1256-0

Determination of fireline intensity by oxygen consumption calorimetry

Paul-Antoine Santoni · Frédéric Morandini · Toussaint Barboni

Received: 23 October 2010 / Accepted: 7 December 2010 / Published online: 24 December 2010

Abstract Fireline intensity is one of the most relevant quantities used in forest fire science. It helps to evaluate the effects of fuel treatment on fire behavior, to establish limits for prescribed burning. It is also used as a quantitative basis to support fire suppression activities. However, its measurement is particularly tricky for different reasons: difficulty in measuring the weight of the fuel consumed in the active fire front, difficulty to evaluate the rate of spread of the fire front, and uncertainty on combustion efficiency. In this study, an innovative and original approach to directly measure the fireline intensity at laboratory scale is proposed. Based on the oxygen consumption calorimetry principle, this methodology is applied here in case of spreading fires, for the first time. It allows for directly measuring the heat released by the fire front. The results are then used to test the famous Byram's formulation that is generally applied to determine the fireline intensity. Combustion efficiency and effective heat of combustion results are provided. The uncertainty and the use of a full scale calorimeter instead of a bench scale calorimeter for this study are discussed.

Keywords Oxygen consumption calorimetry · Heat release rate · Byram's intensity · Combustion efficiency

Abbreviations

AF	*Avena fatua*
FTT	Fire Testing Technology Ltd®
GS	*Genista salzmannii*
HRR	Heat release rate
LSHR	Large scale heat release rate calorimeter
OC	Oxygen consumption
PP	*Pinus pinaster*

P.-A. Santoni (✉) · F. Morandini · T. Barboni
SPE UMR 6134 CNRS, University of Corsica, Campus Grimaldi, BP 52, 20250 Corte, France
e-mail: santoni@univ-corse.fr

Introduction

The concept of fireline intensity was developed by Byram [1] in the 1950s. Frontal fire intensity synonymous with Byram's fireline intensity is the rate of heat release per unit time per unit length of the fire front, regardless of its depth. It is given by

$$I_B = Hwr \quad (1)$$

where I_B (kW m^{-1}) is the fireline intensity, H (kJ kg^{-1}) is the heat yield of the fuel, w (kg m^{-2}) is the weight of the fuel consumed in the active flame front, and r (m s^{-1}) is the rate of spread of the fire. Fireline intensity is a widely used measure in forest fire science: It helps to evaluate the effects of fuel treatment on fire behavior [2], to establish limits for prescribed burning [3], and to assess fire impacts on ecosystems [4]. It is also used as an indicator for the classification of community in terms of risk [5] and as a quantitative basis to support fire suppression activities [6, 7]. However, in that case caution should be exercised, as results obtained for a specific fuel type cannot be generalized to different fuels structures [8].

Although fireline intensity is widely used in fire science as detailed here above, conversely, it has been poorly used as a key parameter to test the new generation of physical [9] and detailed models [10] of fire spread that have been developed during the last 10 years. Such models were tested most often against coarse observations like visible

flame length and rate of spread, and comparison against fireline intensity data was marginal. One can mention of those detailed models which Morvan et al. [11] and Mell et al. [12] have recently tested against intensity for grass fires. The reason for the little use of fireline intensity by modelers may to be found in the difficulty encountered to measure this quantity accurately even at the laboratory scale. As it is in general obtained from the estimates of available fuel energy per unit area of ground and fire spread rate [1], little is known about how well these computed intensities represent the actual rates of energy release. However, this quantity contains in itself the most part of the physics involved in a spreading fire. One can consider that fireline intensity, along with rate of spread and fire front shape, is one of the most relevant information for the test and validation of all types of models of fire spread (from empirical to detailed models). However, care should be taken for its assessment. Very few studies have investigated this quantity [13], and very few methods have been developed to measure it. To our knowledge, Nelson and Adkins [14] are the only ones who attempted developing an alternative method to Byram's formulation for measuring fireline intensity. They used a wind tunnel as a calorimeter to measure the sensible energy released during a fire. Those data were then converted to an average rate of heat release. The comparison between theirs and Byram's intensities showed some divergences that were not fully explained.

Aims

The aim of this study is to investigate fireline intensity at the laboratory scale by means of oxygen consumption (OC) calorimetry and to test Byram's formulation. Effective heat of combustion and combustion efficiency are also discussed. OC calorimetry which has been applied with great success in the fire safety community is used here to understand the dynamics of spreading fires across litters of pine needles, straw, and broom. Litter is a clear fire hazard by providing a continuous fuel matrix across the forest floor that sustains fire spread for a great extent in shrub.A large scale heat release rate (LSHR) calorimeter was used to measure the heat release rate (HRR) of the fire front. The measured HRR corresponds directly to the fireline intensity for fire front of one meter width. The HRR of a fuel is one of the most important parameters for understanding combustion process and fire characteristics [15]. One can question in this study the use of a full scale LSHR calorimeter and not a bench scale calorimeter such as the cone calorimeter [16] or the Fire Propagation Apparatus [17]. Bench scale test method has been widely used to quantify combustion efficiency and effective heat of combustion for different materials like wood [18]. However, little is known on wildland fuels. Recent studies conducted with bench scale calorimeter started with the effort of using calorimetric tools to understand better the burning of wildland fuels [19, 20]. The test conditions allowed the internal porous fuel bed characteristics to be examined. The results indicated that the transport processes inside the fuel bed have a significant impact on the combustion dynamics within the porous bed. Two reasons lead us to the preferred use of a full scale calorimeter instead of a bench scale one. First, as both methods are based on the same measuring principle, the same resulting parameters could be calculated only if a mathematical model that uses cone calorimeter data as input and predicts the heat release in large scale test exists. For some categories of objects, such models have been developed. However, the available categories are few, and such a model has not been developed for wildland fuels. Second, the porous aspect of wildland fuel imposes a constraint that the bench scale cannot always meet for certain fuels and fuel loads. Even for litter which is the most compact wildland fuel, typical layer found in forests are thicker than the 50-mm thickness of the samples used in bench scale. Hence, using a sample representative (not compacted) of the wildland fuel with a reasonable mass leads to a thickness greater than 50 mm. Bench scale calorimeter can thus be used only for litter with low fuel load [20]. Another aspect concerns the holder effect on the porous sample, which is avoided in the full scale calorimeter. Furthermore, if one wants to extend this study to shrubs for which the packing ratio is ten times lower than for litters, then bench scales calorimeters are unusable [21]. Thus, using a bench-scale HRR apparatus is not always enough for comprehensive studies of fires. In the case of this study, it is necessary to study the HRRs of objects in their full scale [22].

Previous considerations

Some comments on Byram's formulation are made as follows:

In Byram's formulation (Eq. 1), fireline intensity is calculated directly by the product of the three variables H, w and r. Some comments given here about this approach can lead to an overestimation of fire intensity. First, it should be mentioned that this method refers to a quasi-steady linear fire front. However, the fire front often takes a narrow shape at the head under wind and/or slope condition, and rate of spread is rarely constant. Then, it is extremely difficult to determine precisely the fuel consumption in the active flaming zone which is the zone at the fire's edge where solid flame is maintained (Fig. 1). Hence, the fuel loadings used are based on total consumption rather than flaming combustion only [13]. In

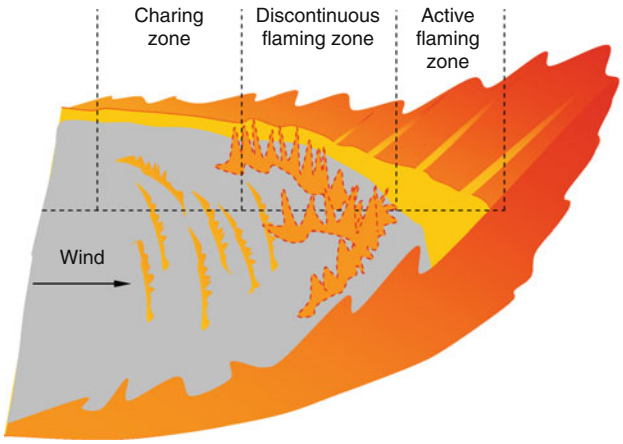

Fig. 1 Sketch of a spreading fire front to illustrate the different zones of heat release

other words, since fuel requires time to burn, the measured heat released is not confined to the flaming leading edge of the fire front but is extended back through the width of the strip in which char combustion is also taking place.

In Eq. 1, the heat yield H is obtained from the net (or low) heat of combustion value $\Delta H_{c,net}$, adapted to the fuel moisture content:

$$H = \Delta H_{c,net} - L_M \times p_M \quad (2)$$

where L_M (24 kJ kg^{-1} [1, 23]) is the heat required to separate the bound water from the fuel and to vaporize the water in the fuel, and p_M is the moisture content percentage point based on dry fuel. The value of the net heat of combustion is derived from the high (or gross) heat of combustion value $\Delta H_{c,gross}$ to take into account the latent heat absorbed when the water of reaction is vaporized. It is given by

$$\Delta H_{c,net} = \Delta H_{c,gross} - L_V \times m_{H_2O} \quad (3)$$

where $L_V = 2257$ kJ kg^{-1} is the latent heat of vaporization of water and m_{H_2O} is the mass of water released during the combustion of 1 kg of fuel. The $\Delta H_{c,gross}$ is usually determined from measurement by oxygen bomb calorimetry.

Measure of the HRR by oxygen consumption calorimetry

Some considerations on the oxygen consumption calorimetry principle

The OC calorimetry is the most common measurement methods used for determining the HRR in kW. HRR which describes the fire size of burning materials is a fundamental parameter that is essential to estimate fire hazards and design fire protection systems [24, 25]. Regarding its use in forest fire science, it should be recalled that HRR and the derived quantities like fireline intensity (kW m^{-1}) and more precisely reaction intensity (kW m^{-2}) are used to model the heat source in some fire spread modeling approaches [26]. The OC calorimetry principle is based on the assumption that the amount of heat released per unit mass of consumed oxygen is approximately constant for most common burning materials containing C, H, and O [27]. Thus, the HRR can be approximated by measuring the oxygen deficit in the exhaust gas flow of burning materials. The key parameters needed to determine HRR are the exhaust mass flow rate and the oxygen depletion. These values are typically determined from real time measurements of velocity, temperature, and species concentration in the exhaust duct flow of a calorimeter.

LSHR calorimeter

The HRR measurements based on OC calorimetry were conducted using the newly installed 1 MW LSHR calorimeter (3 m × 3 m hood) at the University of Corsica. Although this calorimeter has a maximum capacity of 1 MW, it is typically used for fires less than 500 kW to prevent flames from entering the duct. Figure 2 shows the Open-burning HHR Calorimeter with a combustion bench inside. This experimental arrangement is categorized in the Furniture Calorimeters group [28]. It was supplied by Fire Testing Technology Ltd®. The mass loss rate is measured and the exhaust gases are analyzed for composition, temperature, optical obscuration, and flow speed with a bi-directional probe. The HRR calculation uses representative values of measured quantities at the sampling position in the exhaust duct. In order to validate the whole installation and reduce the measurement

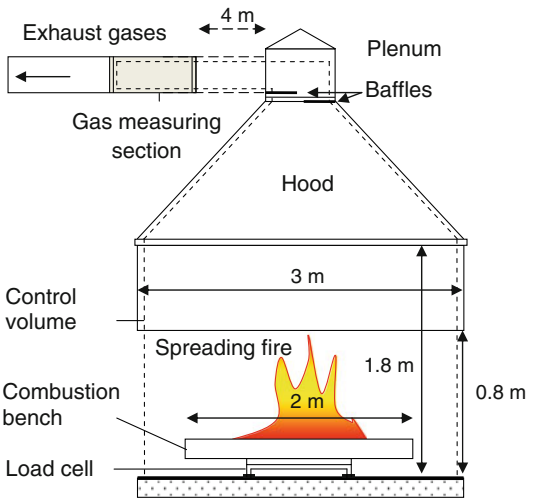

Fig. 2 Overview of the large scale heat release (LSHR) calorimeter with the combustion bench

uncertainty, a calibration procedure with a propane burner is required. A software allows the display of nearly real-time HRRs with corrections for sampling/instrumental delay and response times.

Basic equations

The measurement of exhaust flow velocity and gas volume fractions were used to determine the HRR based on the formulation derived by Parker [29]. When estimating the HRR of a reaction from the chemical species concentration, the main hypothesis lays in the knowledge of the evolution of the combustion gases during the reaction. The combustion of a vegetation species was represented by the stoechiometric reaction for the complete combustion of a chemical compound $C_xH_yO_z$, given by

$$C_xH_yO_z + \left(x + \frac{y}{4} - \frac{z}{2}\right)(O_2 + 3.76N_2) \rightarrow xCO_2 + \frac{y}{2}H_2O + 3.76\left(x + \frac{y}{4} - \frac{z}{2}\right)N_2 \quad (4)$$

The main simplifying assumptions are the following. The amount of energy released by complete combustion per unit mass of oxygen consumed is taken constant for a given fuel for flaming and smoldering. However, these values differ from one vegetation species to the others. The generic value of Huggett's average ($E = 13.1$ MJ kg^{-1} of O_2 [27]) in not used to improve the accuracy of the measurement (see next section); all the gases are considered to behave as ideal gases; the analyzed gas is defined by its composition in O_2, CO_2, H_2O, and N_2. All the other gases are lumped into N_2. The gases are measured on a dry basis. Water vapor is removed because the analyzers cannot handle wet mixtures. Thus, the mole fraction of gases in air is derived from the analyzers' measurements and from air humidity. For instance, the mole fraction of oxygen in air is given by

$$X_{O_2} = (1 - X_{H_2O})X^{a}_{O_2} \quad (5)$$

where superscript "a" denotes the mole fraction in the analyzers. The OC principle is expressed as

$$\dot{q} = E\left(\dot{n}^{\circ}_{O_2} - \dot{n}_{O_2}\right)W_{O_2} \quad (6)$$

where $\dot{q}$ is the HRR, $\dot{n}^{\circ}_{O_2}$ and $\dot{n}_{O_2}$ represent, respectively, the molar flow rates of O_2 in incoming air and in the exhaust duct, and W_{O_2} is the molecular weight of oxygen. The volume flow rate of incoming air, referred to standard conditions is given by

$$\dot{V}_a = \frac{\dot{n}^{\circ}_{O_2} W_{air}}{X^{\circ}_{O_2}\,\rho_0} \quad (7)$$

where $X^{\circ}_{O_2}$ is the molar fraction of O_2 in incoming air, and W_{air} is the molecular weight of dry air at 25 °C and 1 atm. The oxygen depletion factor is introduced for convenience. It is given by

$$\phi = \frac{\dot{n}^{\circ}_{O_2} - \dot{n}_{O_2}}{\dot{n}^{\circ}_{O_2}} \quad (8)$$

Combining Eqs. 6–8, one obtains

$$\dot{q} = \frac{E\rho_0 W_{O_2}}{W_{air}} X^{\circ}_{O_2}\phi\dot{V}_a \quad (9)$$

Unfortunately, in an open system, not the incoming air flow rate, but the flow rate in the exhaust duct $\dot{V}_s$ is measured. A relationship between $\dot{V}_a$ and $\dot{V}_s$ is obtained after some development [29]. Finally, the HRR is given by the three following relations:

$$\dot{q} = \frac{E\rho_0 W_{O_2}}{W_{air}}\left(1 - X^{\circ}_{H_2O}\right)X^{a\circ}_{O_2}\dot{V}_{s,298}\left(\frac{\phi}{(1-\phi) + \alpha\phi}\right) \quad (10)$$

$$\dot{V}_{s,298} = 22.4A\frac{k_t}{k_p}\sqrt{\frac{\Delta P}{T_s}} \quad (11)$$

$$\phi = \frac{X^{a\circ}_{O_2}\left(1 - X^{a}_{CO_2}\right) - X^{a}_{O_2}\left(1 - X^{a\circ}_{CO_2}\right)}{X^{a\circ}_{O_2}\left(1 - X^{a}_{CO_2} - X^{a}_{O_2}\right)} \quad (12)$$

where X denotes the molar fraction, ρ_0 is the density of dry air at 298 K and 1 atm, $\dot{V}_{s,298}$ is the standard flow rate in the exhaust duct, and $\alpha = 1.105$ is the expansion factor for the fraction of the air that was depleted of its oxygen. The superscript "°" is for the incoming air. A is the cross-sectional area of the duct, k_t is a constant determined via the calibration with a propane burner, $k_p = 1.108$ for a bi-directional probe, ΔP is the pressure drop across the bi-directional probe, and T_s is the gas temperature in the duct.

Uncertainty of HRR measurement from LSHR

The HRR is computed from many variables and each variable has a corresponding uncertainty which reflects in the mathematical function giving the HRR. The relative expanded uncertainty on HRR is obtained from the uncertainty propagation. Two types of uncertainties are generally used [30]: Type A uncertainties pertain to random variable and are estimated on the basis of statistics analysis of repeat measurements (such as the standard deviation about the mean). The others, designated as Type B are based on scientific judgment or specifications. However, for large scale apparatus, one can also mention random effects on fire growth that can affect the repeatability of the tests [31] and increase the uncertainty. The LSHR used in this study was installed by Fire Testing Technology Ltd® (FTT). The instrumentation package supplied are those corresponding to the Room Corner Test [32] for which Axelsson et al. [33] have analyzed the

uncertainty considering individual sources of errors for rate of heat release measurements. The combined expanded uncertainty was provided with a coverage factor of 2, giving a confidence level of 95%. Uncertainty of ±10.6% at 150 kW level was reported in that study. The uncertainties of the oxygen concentration measurement, followed by the heat of combustion factor E and the mass flow rate measurement were identified as the major sources of uncertainty. The following precautions were taken to reduce the measurement uncertainties. Analyzers were developed specifically for FTT Calorimeters, incorporating an enhanced Servomex 4100 featuring a high stability temperature controlled paramagnetic oxygen sensor with flow control and by-pass for fast response. The accuracy of the exhaust duct volume flow measurement was improved by calibrating the bi-directional probes in a controlled flow. The variation in HRRs due to the variation in E is given by

$$\delta\dot{q} = \frac{\partial\dot{q}}{\partial E}\delta E \tag{13}$$

where

$$\frac{\delta\dot{q}}{\delta E} = \frac{\rho_0 W_{O_2}}{W_{air}}\left(1 - X^{\circ}_{H_2O}\right)X^{a\circ}_{O_2}\dot{V}_{s,298}\left(\frac{\phi}{(1-\phi)+\alpha\phi}\right) \tag{14}$$

When the fuel composition is known, a more accurate value for E can be determined [34]. Following the assumption of the stoechiometric reaction given in Eq. 4 (valid since the experiments were conducted under well-ventilated conditions), the OC calorimetry energy constants can be estimated from the fuels ultimate analysis and low heat of combustion

$$E^{fuel}_{st} = \frac{\Delta H^{fuel}_{c,net} W_{fuel}}{n_{O_2} W_{O_2}} \tag{15}$$

where $n_{O_2} = x + y/4 - z/2$ (see Eq. 4) and W_{fuel} is the molecular weight of the fuel. The values of E for the vegetation species considered in this study are given in the next section.

Experimental methodology to measure the fireline intensity by OC

Calibration of the LSHR

Because the calculation of HRR requires a large number of individual measurements, it is essential to have an independent confirmation of measurement accuracy. This calibration is accomplished by burning an accurately measured flow of gas having a well-defined heat of combustion. In order to reduce the uncertainty on the calibration, a burner with good repeatability was used. It was provided by FTT® and constructed according to ISO 9705

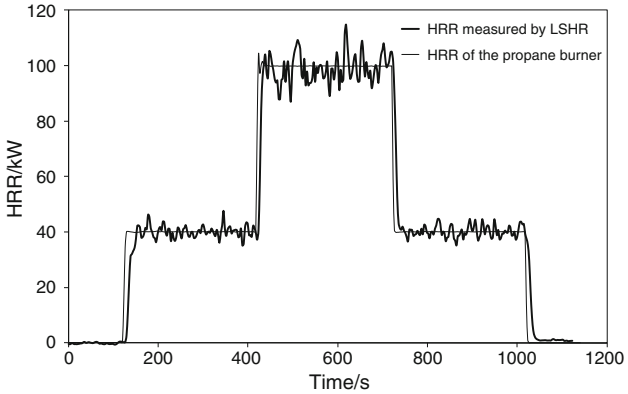

Fig. 3 Calibration of the LSHR with propane gas at levels of 40–100–40 kW

[32] Annexes A1 and A2 complete with gas train. A mass flow controller with digital display controls the gas flow, and the gas controls include an auto-ignition unit. The burner can produce flows corresponding to a range of HRRs from 10 kW to over 300 kW. Different increments can be specified by the user (see Fig. 3). The burner and flow system are configured to use propane gas. Owing to the HRR expected for the vegetative fuel bed used in this study, the calibration of the LSHR hood and ducting was conducted by burning propane gas at levels of 40–100–40 kW. Figure 3 is a graphical example of a fire test performed with the calibration burner.

The results of the LSHR measure should closely agree with the burner output. A comparison factor is determined from the ratio of the oxygen calorimetry and burner HRRs. It is used as a validation and quality control factor for the calorimetry. When this factor is observed to fall outside predetermined bounds, it is time to troubleshoot the systems, calorimetry, and calibration burner. The relative agreement between the OC calorimetry and the burner output was better than 0.97 for the entire range of the HRRs considered. The authors paid particular attention to the location of the burner under the hood. Indeed, owing to the use of the LSHR for spreading fire (see next section), the burner was positioned at three different locations under the hood: center of the hood and at 0.5 m front and back along the expected spread. For each location, three repetitions were done. The aim was to verify that the location of the fire does not change the flow profile at the sampling location within the duct. The following value for the coefficient, viz., $k_t = 0.804 \pm 0.004$ (Eq. 11) was obtained, which induces an uncertainty on HRR of 0.5%.

Measurement of the fireline intensity

Three species of vegetation were considered in these test fires: *Pinus pinaster* (PP) needles, *Avena fatua* (AF) straw

(wild oats), and *Genista salzmannii* (GS) spines (an endemic broom). Experimental fires were conducted under no slope and without wind for line-ignition fires on a combustion table located inside the calorimeter hood. The table is an air-entrained concrete plate of 2 m long and 2 m wide, placed on a load cell to measure the mass loss over time during the fire test. The bed of fuel occupies only the central part of the tray. Different fuel loads were considered. Different sizes of fuel bed were used (0.9 m × 1.1 m, 1 m × 1.5 m and 1 m × 2 m), and different moisture contents on dry basis were considered (4–7%). The different fuels were scattered uniformly on the tray to obtain homogeneous beds. To ensure fast and linear ignition, a small amount of alcohol and a flame torch were used (see Fig. 4).

The fuel species present different characteristics such as surface-to-volume ratio, density, heat of combustion, and chemical compounds. These properties are among the main parameters that are used in detailed physical models to describe the influence of fuel species on the combustion dynamics [11]. A proper characterization of those fuels was done instead of using classical literature values to improve the precision and improve the analysis, and also because the results presented in this study can be used to test fire spread models. The range of fuel bed properties for each vegetation species considered in this study are provided in Table 1 where w, δ, ρ, σ, and β represent, respectively, the fuel load, the depth of the fuel bed, the density of the particles, the surface-to-volume ratio of the particles, and the packing ratio of the fuel bed. The net heat of combustion $\Delta H_{c,net}$ values were derived from the gross heat of combustion values $\Delta H_{c,gross}$, measured in an oxygen bomb calorimeter following the standard AFNOR NF EN 14918 [35]. The surface-to-volume ratio and density were measured following the methodology proposed by Moro [36]. The moisture content was determined by drying the species in an oven at 60 °C for 24 h. The fuel bed height was measured in each test leading to the apparent volume of the fuel bed and to the porosity $\beta = w/(\rho\delta)$. The bulk density was 8.6 kg m^{-3} for AF, 25 kg m^{-3} for GS, and 20 and 17 kg m^{-3} each for PPs with loads of 0.6 and 1.2 kg m^{-2}. The ambient temperature and relative humidity ranged, respectively, from 18 to 21 °C and from 35 to 49% for the entire range of tests.

Fig. 4 Linear ignition for a 1 m × 1.5 m bed of *Pinus pinaster* needles inside the LSHR hood

The HRR was measured during the spreading across the fuel beds under the LSHR hood. The fire fronts remained quasi linear during the entire spreads and exhibited a weak curvature on the flanks when reaching the end of the combustion bench. The fireline intensity obtained by OC calorimetry denoted I_{OC}, correspond directly to the measured HRR for fire front with 1-m width. For the fuel bed of smaller width, W, the fireline intensity is given by

$$I_{OC} = \dot{q}/W \tag{16}$$

Results and discussion

Uncertainty of HRR measurement for spreading fires

In order to verify that the location of the fire does not change the flow profile at the sampling location within the duct, some experiments were carried out in two directions: from one edge of the bench toward the other edge at first, and then in reverse. No significant modification in the resulting HRR was observed. At least, three repetitions were made to collect reliable data for each fuel and fuel load. As an example, Fig. 5 displays the typical combustion behavior for a set of test runs (three repetitions) conducted across fuel beds of PP needles with a load of 0.6 kg m^{-2} (see Table 1 for fuel bed properties). Repeatable estimates for the HRRs can be seen. As HRR is calculated using O_2 and CO_2, the repeatability of the HRR is also an indication of the repeatability of all the measured gas concentrations. One can also mention that the random effects on fire growth that can affect the repeatability of the tests [31] do not influence the general tendency of the HRR. In Fig. 5, for instance, it can be seen that although test 1 shows differences in comparison with tests 2 and 3 between the first and second minute, the HRR curves are overlapped during the rest of the spreading. The duration, the ignition, and the extinction were almost the same for the three replicates. The drastic increases and decreases in HRR at the beginning and at the end of the experiments follow the same tendency. In addition, although the HRR was fluctuating randomly during the spread, conversely those fluctuations are clearly around an average constant value that corresponds to a quasi-steady state.

As mentioned in the previous section, the values of the OC calorimetry energy constants, E, were calculated (Eq. 15) for each fuel to reduce the uncertainty on HRR (Eq. 14). Calculation of E necessitates knowing the fuel

Table 1 Range of fuel bed properties of the vegetation species

Species	Symbol	$\Delta H_{c,net}$/kJ kg^{-1}	σ/m^{-1}	ρ/kg m^{-3}	p_M/%	w/kg m^{-2}	δ/cm	$\beta \times 10^{-3}$
Avena fatua	AF	17091	2394	287	4–7	0.6	7	30
Genista salzmannii	GS	20645	3100	967	5	0.9	3.5	26
Pinus pinaster	PP	20411	3057	511	3–5	0.6–1.2	3–7	39–33

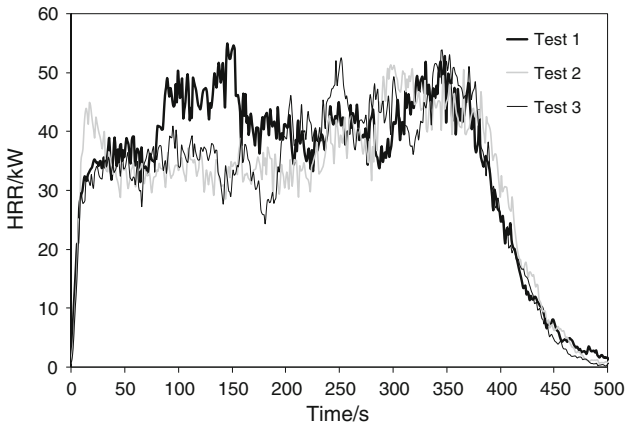

Fig. 5 HRRs for three replicates of fires across fuel beds (1 m × 1.5 m) of PP with a load of 0.6 kg m^{-2}

ultimate analysis (see Eq. 4). Ultimate analysis (in mol) is given in Table 2, besides the values of E for the different vegetation species.

The variation from the standard E value (δE) is an increase by 2.9% for GS, 6.7% for PP, and 9.8% for AF. According to Eq. 13, those variations will affect HRR calculations. HRR for fire spreading across AF and GS fuel beds obtained from both Huggett's average and calculated values of E, as well as the variation in HRR calculated from Eqs. 13 and 14 are displayed in Fig. 6a and b. Using the specific E values for each fuel instead of the average ones improves the precision on the HRR calculation. The HRR is underestimated by the use of the average constant for the three species. However, as denoted by these figures, the uncertainty is different for the different fuels. Although negligible for GS, it is important for AF. Using the same energy constant for different fuel species can lead to wrong tendencies since the HRR which was calculated using the average constant is not underestimated in the same proportion according to the species. Another source of

Table 2 Ultimate analysis (mol units) and energy constants estimated of the vegetation species

Species	Symbol	x/mol	y/mol	z/mol	α	E_{st}/MJ kg^{-1}
Avena fatua	AF	3.66	5.74	2.77	1.16	14.39
Genista salzmannii	GS	4.26	6.72	2.32	1.12	13.48
Pinus pinaster	PP	4.15	6.65	2.51	1.13	13.98

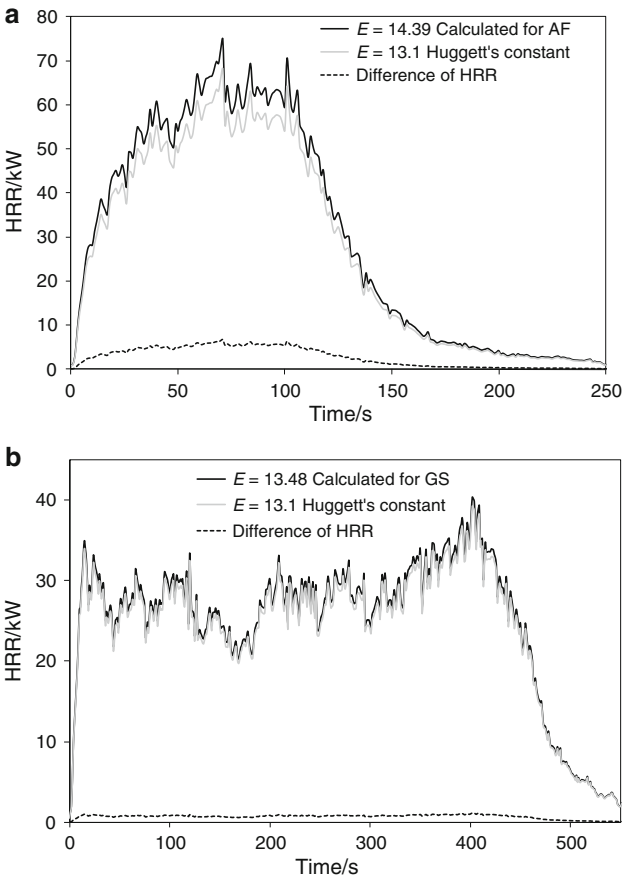

Fig. 6 HRR curves using Huggett's constant and E calculated, and ΔHRR for fire spread across fuel beds of **a** AF (0.9 m × 1 m) for a load of 0.6 kg m^{-2}, **b** GS (1 m × 1 m) for a load of 0.9 kg m^{-2}

uncertainty for the measurement of HRR mentioned by Babrauskas [28] is the expansion factor α. α is given by the following relationship:

$$\alpha = 1 + (\beta - 1)X_{O_2}^{\circ} \tag{17}$$

with

$$\beta = \frac{4x + 2y}{4x + y - 2z} \tag{18}$$

The interested reader is referred to [29] for details. An average value $\alpha = 1.105$ is usually used for unknown fuels. The values of α calculated for each fuel are given in Table 2. The effect of α on the calculation of the HRR was negligible in the studied case for the three vegetation species.

Fireline intensity for quasi-steady fires

Figures 7 and 8 display some examples of the curves of fireline intensity for fires spreading across PP for two loads (0.6 and 1.2 kg m^{-2}). The corresponding mass loss over time is superimposed on the HRR curves. Since the fire front was of 1-m width, the value of fireline intensity (kW m^{-1}) is equal to HRR. For all the experiments, a first peak of HRR at approximately 40 kW was observed. It corresponds to the heat released by the burning of alcohol during the ignition. Then, depending on the fuel load, it could be observed that a quasi-steady state was achieved more or less quickly. The highest the fuel load, the latest the steady state was reached. However, the steady state lasted enough to allow us calculating relevant averaged quantities for rate of spread, mass loss rate, and HRR. During these time intervals (see Figs. 7, 8), it was further observed that constant rates of spread, constant rates of mass loss, and roughly constant HRRs were obtained. Owing to the turbulence in the flame, it can be seen (Figs. 7, 8) that the HRR is not as smooth as the mass loss,

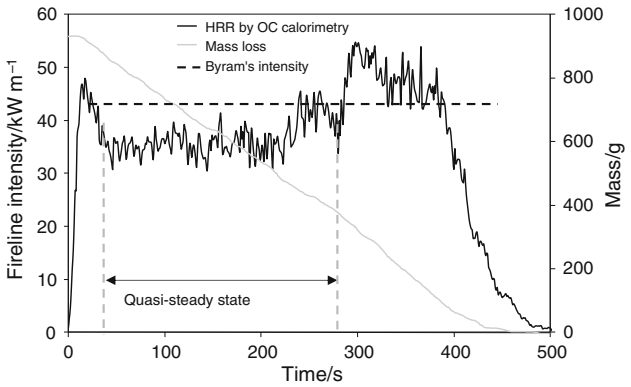

Fig. 7 Fireline intensity and mass loss over time for fire spread across a fuel bed of PP (1 m × 1.5 m) for a load of 0.6 kg m^{-2}

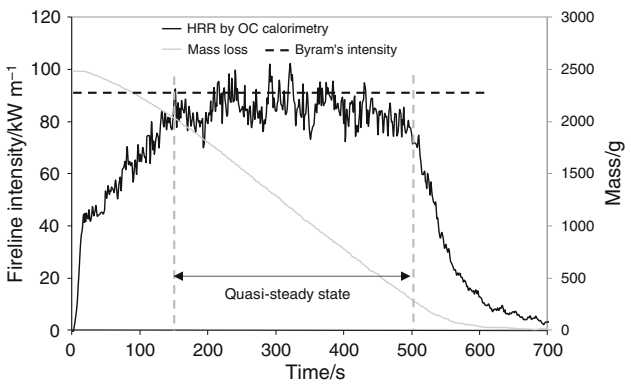

Fig. 8 Fireline intensity and mass loss over time for fire spread across a fuel bed of PP (1 m × 2 m) for a load of 1.2 kg m^{-2}

for all the experiments. For the two tests provided in this study, the mean rates of spread were 0.37 and 0.4 cm s^{-1}, the mean rates of mass loss were −2.16 and −4.45 g s^{-1}, and the mean fireline intensities were 36 and 84 kW, respectively, for PPs with loads of 0.6 kg m^{-2} and 1.2 kg m^{-2}. The figures for AF and GS fuel beds are similar, thus they are not provided for the sake of brevity. The main results for AG and GS are the mean rates of spread were 0.87 and 0.24 cm s^{-1}, the mean rates of mass loss were −3.81 and −1.64 g s^{-1}, and the mean fireline intensities were 58.5 and 28.6 kW, respectively. Considering the fuel bed properties (see Table 1 and "Experimental methodology to measure the fireline intensity by OC" section), the fuel bulk density is the main parameter that differs from one fuel bed to the other. One can assume that the burning rate of the fuel bed, hence the fireline intensity are mainly related to the bulk density. The lowest the bulk density, the highest are the rate of spread, the rate of mass loss, and the fireline intensity.

Test of Byram's formulation to measure the fireline intensity

The results presented in the previous section guarantee that sound steady-state regimes in energy release that correspond effectively to constant rate of mass loss and constant rate of spread are obtained. The authors are thus able to test Byram's formulation to assess fireline intensity for quasi-steady spreading fires. The Byram's intensities measured in this study's experiments ranged from 17 to 100 kW m^{-1}. Before confronting these results to OC measurements, it is important to recall the context of Byram's measurements of fireline intensity [1] to show that the comparison is relevant. Byram's study [1] was conducted for small test fires. The observations were mostly for fires backing into the wind (34 tests) rather than burning with the wind (5 tests), because the test fires were part of a prescribed burning study. The light fuels were fairly uniform mixtures of grass and pine needles. The fuel load ranged from 0.49 to 0.730 kg m^{-2}. The rate of spread ranged from 0.9 to 1.8 cm s^{-1} for backing fires, and their intensities ranged from about 65 to 201 kW m^{-1}.

Figure 9 shows OC calorimetry intensities versus Byram's intensities for the whole set of experiments conducted in our study. It can be seen that Byram's formulation I_B, overestimates I_{OC}, the fireline intensity measured by OC calorimetry. The ratio between both formulations given by the linear regression is $I_{OC}/I_B \approx 0.84$. If one considers this ratio by fuel beds, then it is noted that the mean values range from 0.77 to 0.87 (see Table 3). Byram's intensities values are also plotted on Figs. 7 and 8 for PP fuel beds to compare with these results.

Two reasons may explain the difference between Byram's formulation and OC calorimetry results. The first one

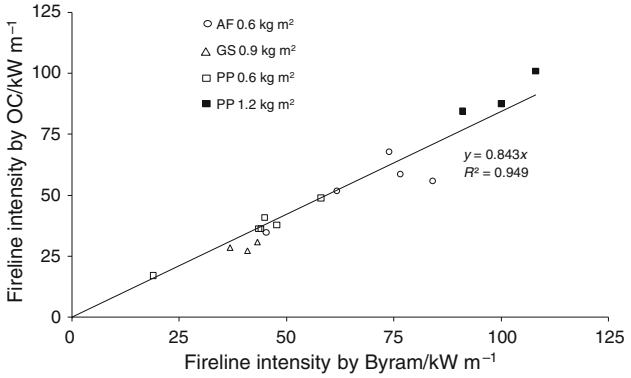

Fig. 9 OC calorimetry Fireline intensity versus Byram's intensity for all the test fires

Table 3 Ratio of OC calorimetry intensity to Byram's intensity

Species	AF/0.6 kg m^{-2}	GS/0.9 kg m^{-2}	PP/0.6 kg m^{-2}	PP/1.2 kg m^{-2}
I_{OC}/I_B	0.79	0.77	0.82	0.87

is due to the methodology adopted to apply Byram's formulation. As mentioned previously, the fire fronts remained quasi linear during the whole range of spreads but exhibited a weak curvature on the flanks. This shape leads to a slight overestimation of the burned load when the fire reaches the end of the combustion bench. The second one is due to combustion efficiency that is overestimated in Byram's formulation. Indeed, Eq. 1 considered the heat yield H (see Eq. 2), while the combustion is incomplete. In order to support this conclusion, an analysis on the combustion efficiency for the whole set of fire tests will be considered in the next subsection .

Effective heat of combustion and combustion efficiency

The effective heat of combustion H_{eff} is representative for real fire conditions where there is unlimited availability of air. A global effective heat of combustion was determined for each test, i, by dividing the total heat released by the total mass lost during the quasi-steady stage, as determined from the load cell (accuracy of 1 g). For instance, for AF

$$H_{eff}^{AF,i} = \int_{T_{in}}^{T_{fi}} \dot{q}\,dt/(m_{in} - m_{fi}) \tag{19}$$

where subscript "in" and superscript "fi" are for initial and final time of steady stage, respectively. Then, for each species and each load, a mean effective heat of combustion was calculated by averaging the global effective heat of combustion obtained for the set of tests. The mean effective heats of combusiton are provided in Table 4 for the whole species and loads.

Table 4 Effective heat of combustion and combustion efficiency

Species	AF/ 0.6 kg m^{-2}	GS/ 0.9 kg m^{-2}	PP/ 0.6 kg m^{-2}	PP/ 1.2 kg m^{-2}
$\overline{H_{eff}}$/kJ kg^{-1}	14579	17133	18197	17364
χ	0.9	0.88	0.94	0.9

$$\overline{H_{eff}^{AF}} = \frac{1}{i}\sum_{i=1}^{N} H_{eff}^{AF,i} \tag{20}$$

The combustion efficiency χ which represents the ratio between the effective heat of combustion and the net heat of combustion, $\chi = H_{eff}/\Delta H_{c,net}$ was calculated for each fuel bed. A modified but more appropriate formulation for χ, was used for taking into account the fuel moisture content of the fuels studied:

$$\chi = H_{eff}/H \tag{21}$$

Table 4 displays the mean values of χ obtained for the test fires conducted across the different fuel beds.

The above results corroborate the conclusions of the previous section. Byram's formulation overestimate the heat release as it considers a complete combustion. A modified Byram's formulation for fireline intensity considering combustion efficiency could be given by

$$I_{BM} = \chi H w r \tag{22}$$

Effective heat of combustion was also measured by Babrauskas [21] for flaming combustion of Douglas-fir (Christmas trees, 2.0 m tall). This last study concerned mainly the influence of moisture content on effective heat of combustion. His results at low moisture content are consistent with those of this study. He had obtained $H_{eff} = 16.52$ MJ kg^{-1} for dry foliar moisture while the net heat of combustion was $\Delta H_{c,net} = 18.3$ MJ kg^{-1}. Hence, $\chi = 0.9$ in his case. In the studied case, however, a slight difference between the values of χ for the different fuel beds was observed. The average value when considering all the fuel beds is 0.9. The values of combustion efficiency obtained in this study are in agreement with those provided by other investigators for free burn test [37]. The results of this study demonstrate that actual combustion processes vary considerably from out-of-context laboratory estimates, for example, heat of combustion determinations using oxygen bomb calorimetry rather than oxygen depletion calorimetry during free burning. In fact, the bomb calorimeter measures the complete heat of combustion, $\Delta H_{c,gross}$, where the fuel is completely combusted under high pressure in pure oxygen. In a free burn test, the fuel is burned with unlimited access to air, but some of the volatiles do not burn completely, leaving, for example, CO, soot, and unburnt hydrocarbons, containing further potential energy. Therefore, H_{eff} is lower than H.

Conclusions

The main contributions of this study can be summarized as follows:

- A methodology was proposed to measure fireline intensity for fire spreading across litters of vegetation species with a full scale heat release calorimeter. The use of OC calorimetry was improved by a complete characterization of the fuels and a calculation of the appropriate OC energy constants for each fuel species. Using those values instead of the Huggett's average constant improves the HRR calculation uncertainty.
- At this scale, it was shown that Byram's formulation overestimates the fireline intensity from approximately 13–23% depending on the species. A more appropriate formulation for fireline intensity calculation should thus consider combustion efficiency.
- Actual combustion processes vary considerably from out-of-context laboratory estimates, for example, heat of combustion determinations using oxygen bomb calorimetry rather than oxygen depletion calorimetry during free burning.

Although this study was conducted at laboratory scale, the results are relevant for the purpose of testing fire spread models that will be used at field scale. Indeed, fire spread models are often developed in two stages. A first stage requires a comparison between sound thermodynamic data measured in experiments carried out at laboratory scale to validate the structure of the model. Then, a second stage is necessary to fit a model's parameters at field scale by comparison of a model's prediction with coarse fire behavior descriptors, like rate of spread. The authors provide here for the first time some measures of the heat release by spreading fires. Those results will be useful for modelers who aim at testing combustion mechanisms or source term used in their detailed models [10–12] of fire spread.

Acknowledgements This study was carried out within the scope of project PROTERINA-C supported by the EU under the Thematic 3 of the Operational Program Italia/France Maritime 2007–2013, contract (#G25I08000120007).

References

1. Byram GM. Combustion of forest fuels. In: Davis KP, editor. Forest fire: control and use. New York: Mc Graw-Hill; 1959. p. 61–89.
2. Fites JA, Henson C. Real-time evaluation of effects of fuel-treatments and other previous land management activities on fire behavior during wildfires. Report of the Joint fires science rapid response project. US Forest Service; 2004. p. 1–13.
3. McArthur AG. Control burning in eucalypt forests. Comm. Aust. For. Timb. Bur. Leafl. No. 80; 1962.
4. Hammil KA, Bradstock RA. Remote sensing of fire severity in Blue Mountains: influence of vegetation type and inferring fire intensity. Int J Wildland Fire. 2006;15:213–26.
5. De Luis M, Baeza MJ, Raventos J, Gonzales-Hidalgo JC. Fuel characteristics and fire behaviour in mature Mediterranean gorse shrubland. Int J Wildland Fire. 2004;13:79–87.
6. Alexander ME, De Groot WJ. Fire behavior in jack pine stands as related to the Canadian Forest Fire Weather Index System. Edmonton: Can. For. Serv., North. For. Cent.; 1988. Poster.
7. Palheiro PM, Fernandes P, Cruz MG. A fire behaviour-based fire danger classification for maritime pine stands: comparison of two approaches. In: Viegas DX, editor. Proc. V Int. Conf. on Forest Fire Research; 2006. CD-ROM.
8. Cheney NP. Quantifying bushfires. Math Comput Model. 1990; 13:9–15.
9. Balbi JH, Rossi JL, Marcelli T, Santoni PA. A 3D physical real-time model of surface fires across fuel beds. Combust Sci Technol. 2007;179:2511–37.
10. Zhou X, Mahalingam S, Weise D. Experimental study and large eddy simulation of effect of terrain slope on marginal burning in shrub fuel beds. Proc Combust Inst. 2007;31:2547–55.
11. Morvan D, Meradji S, Accary G. Physical modelling of fire spread in grasslands. Fire Safety J. 2008;44:50–61.
12. Mell WE, Jenkins MA, Gould J, Cheney P. A physics based approach to modeling grassland fires. Int J Wildland Fire. 2007;16:1–22.
13. Alexander ME. Calculating and interpreting forest fire intensities. Can J Bot. 1982;60:349–57.
14. Nelson RM, Adkins CW. Flame characteristics of wind-driven surface fires. Can J For Res. 1986;16:1293–300.
15. Babrauskas V, Peacock RD. Heat release rate: the single most important variable in fire hazard. Fire Safety J. 1992;18: 255–92.
16. International Standard. Fire tests—reaction to fire—part 1: rate of heat release from building products (cone calorimeter method), ISO 5660-1:1993. Geneva: International Organization for Standardization; 1993.
17. ASTM E2058-03. Standard test method for measurement of synthetic material flammability using a fire propagation apparatus; 2003.
18. White RH, Dietenberger MA. Fire Safety. Wood handbook—wood as an engineering material. Gen. Tech. Rep. FPL-GTR-113. Madison: U.S. Department of Agriculture, Forest Service, Forest Products Laboratory; 1999. 16 p.
19. Schemel C, Simeoni A, Biteau H, Rivera J, Torero JL. A calorimetric study of wildland fuels. Exp Therm Fluid Sci. 2008; 32(7):1381–9.
20. Bartoli P, Simeoni A, Biteau H, Torero JL, Santoni PA. Determination of the main parameters influencing forest fuel combustion dynamics. Fire Safety J. 2010. doi:10.1016/j.firesaf.2010.05.002.
21. Babrauskas V. Effective heat of combustion for flaming combustion of conifers. Can J For Res. 2006;36:659–63.
22. Babrauskas V, Grayson SJ. Heat release in fires. London: Interscience Communications Ltd; 2009. 623 p.
23. Agueda A, Liodakis S, Pastor E, Planas E. Characterization of the thermal degradation and heat of combustion of *Pinus halepensis* needles treated with ammonium-polyphosphate-based retardants. J Therm Anal Calorim. 2009;98:235–43.
24. Wu Q, Zhang C, Liang R, Wang B. Combustion and thermal properties of epoxy/phenyltrisilanol polyhedral oligomeric silsesquioxane nanocomposites. J Therm Anal Calorim. 2010;100: 1009–15.
25. Kim SC, Bundy MJ. Numerical model of a large-scale oxygen consumption fire calorimeter. J Therm Anal Calorim. 2008;93: 1013–9.

26. Rothermel RC. A mathematical model for predicting fire spread in wildland fuels. USDA For. Serv. Res. Pap. INT-115; 1972.
27. Huggett C. Estimation of the rate of heat release by means of oxygen consumption. J Fire Flammability. 1980;12:61–5.
28. Babrauskas V. Heat release rates. In: Quincy MA, Di Nenno JP, Walton WD, editors. The SFPE handbook of fire protection engineering. 3rd ed. National Fire Protection Association and The Society of Fire Protection Engineers; 2002. p. 1–37.
29. Parker WJ. Calculations of the heat release rate by oxygen consumption for various applications. NBSIR 81-2427-1; 1982.
30. Bryant RA, Mulholland GW. A guide to characterizing heat release rate measurement uncertainty for full-scale fire tests. Fire Mater. 2008;32:121–39.
31. Janssens ML, Measurement needs for fire safety proceedings. In: Proceedings of an International workshop. NISTIR 6527; 2000. p. 186–200.
32. International Standard. Fire tests—full scale room test for surface products, ISO 9705. Geneva: International Organization for Standardization; 1993.
33. Axelsson J, Andersson P, Lönnermark A, Van Hees P, Wetterlund I. Uncertainties in measuring heat and smoke release rates in the Room/Corner test and the SBI. Borås: Swedish National Testing and Research Institute; 2001. 41 p. SP report 2001:04.
34. Biteau H, Steinhaus T, Schemel C, Simeoni A, Marlair G, Bal N, Torero JL. Calculation methods for the heat release rate of materials of unknown composition. In: Fire safety science—proceedings of the ninth international symposium, international association for fire safety science; 2008. p. 1165–76.
35. Biocombustibles solides—détermination du pouvoir calorifique. AFNOR NF EN 14918; 2010.
36. Moro C. Détermination des caractéristiques physiques de particules de quelques espèces forestières méditerranéennes. INRA PIF2006-06; 2006.
37. Karlsson B, Quintiere J. Enclosure fire dynamics. CRC Press LLC; 2000.